Supplemental Information

Creating Measurement-Based Oil and Gas Sector Methane Inventories using Source-Resolved Aerial Surveys

Matthew R. Johnson*, Bradley M. Conrad, David R. Tyner

Energy & Emissions Research Laboratory,
Department of Mechanical and Aerospace Engineering,
Carleton University, Ottawa, ON, Canada, K1S 5B6

*To whom correspondence and material requests should be addressed: Matthew.Johnson@carleton.ca; +1-613-520-2600 ext.4039.

File contains 32 pages, 3 figures, 10 tables

S1 Survey Design and Planning

S1.1 Determination of Active Facilities

The aerial survey was planned using available activity and production data from the British Columbia Oil and Gas Commission (BCOGC) and the PETRINEX reporting system website (Petrinex, 2022a) with the simultaneous objectives of maximizing survey coverage and minimizing sample size uncertainties in the derived emissions inventory. A set of active oil and gas facilities and wells were first identified using Petrinex volumetric monthly production data obtained from BCOGC and supplemental active and suspended facility lists from the Petrinex website. Because publicly available active facility lists are not always accurate or up to date, facilities and wells required to report under the Petrinex system were instead deemed active or inactive based on the existence of reported activity data during the month of the survey. For compressor stations, which do not directly report monthly activity via Petrinex, an initial active count was derived from public activity lists and subsequently checked and updated where necessary based on review of aerial imagery of survey sites (e.g., in cases where images showed all compressors had been removed from the site) and provincial leak detection and repair (LDAR) reporting. As detailed in Table S1, 1,006 facilities within the province of British Columbia (BC) were identified as active during the aerial survey of which 601 (60%) were measured.

The active status of individual wells was also gleaned from Petrinex data where well production volumes are found under one or more unique well identifiers (UWI) linked to facilities reporting to Petrinex. These UWI represent segments of a well and were aggregated to shared surface-holes (wells) using well authorizations (WA) assigned by BCOGC in BIL-194. As detailed in Table S1, this analysis identified 8,995 active wells within the province, of which 904 (10%) were captured in the aerial survey. Wells and associated production equipment (e.g., separators, line heaters, pump buildings, etc.) maybe co-located with facilities on common pad ("on-site wells") or reside at completely separate well-site location ("off-site wells", OSW). Since equipment associated with on-site wells may not be distinguishable from that associated with the facility, aerial measured equipment sources at these locations were assigned to the facility. Within the inventory a well was deemed to be off-site if the wellhead surface location was located in a different land grid location (i.e., legal subdivision or NTS quarter unit) than the facility where it reported production. The majority of wells in British Columbia, 97% (8,729 of 8,995), were considered to be off-site; these constituted ~78% (705 of 904) of surveyed wells.

For facilities and wells appearing in Petrinex there were 22 associated activity codes (Petrinex, 2022b) in the monthly volumetric data which track production, flaring, venting, transfers (receipts and dispositions), storage (injection), and losses (shrinkage and metering differences) of produced and processed fluid volumes, as well as a "shut-in" status. Shut-in facilities and wells in the monthly data are sites that are capable of processing, producing, or injecting but were inactive during an entire reporting month. Shut-in sites may have been active in months prior to the survey and may becoming active again or may ultimately be moved to a suspended status and abandoned. For all results presented in the manuscript, shut-in facilities and wells were conservatively assumed to be non-emitting. However, it is possible that some shut-in sites could remain fully or partially pressurized thus having a potential to emit. Reviewing Table S1, at the time of the survey there were an additional 95 "active" but shut-in facilities (9% increase over the 1006 non-shut-in facilities) and 9978 "active" but shut-in wells (11% increase over the 8995 non-shut-in wells).

To bound the potential impact of these shut-in facilities/wells, the entire inventory analysis was repeated including these facilities as active. As shown below in Table S4 and Table S5, including these sites results in a small increase of 4.1 kt (2.8%) in the total inventory. Most of this difference is a 2.7 kt increase in pneumatic equipment emissions, which could be expected if the pneumatic equipment at these shut-in facilities and wells remains pressurized and emitting at expected steady bleed rates. For this reason, regulatory clarification of what qualifies as shut-in, and if possible, differentiating between pressurized and ready to produce versus sealed at the wellhead, is highly recommended. By contrast, including shut-in facilities and wells in the analysis made little difference in the measured source portion of the inventory (112.9 kt including shut-ins, or a 0.6% increase over the 112.2 kt measured source total presented in the manuscript).

S1.2 Sampling Region and Strata

During the initial survey planning phase, candidate survey location were identified by geo-locating all active facilities and wells in ArcGIS Pro using BCOGC permit data (BCOGC, 2022a, 2022b), land grid locations (Dominion Land Survey legal subdivisions and National Topographic Systems quarter units), and BCOCG surface-hole locations for wells (BCOGC, 2022c). A review of these candidate sites identified a significantly lower facility density in the northern region centered around Fort Nelson, Figure S1. Given the sparseness of facilities and budgetary constraints, the initial set of candidate sites was constrained to a smaller survey region of approximately 46,000 km^2 south of approximately 58°N. Limiting the area covered by the aerial survey was also essential for the feasibility of conducting parallel on-site follow-up investigations of detected sources (Johnson et al., 2022).

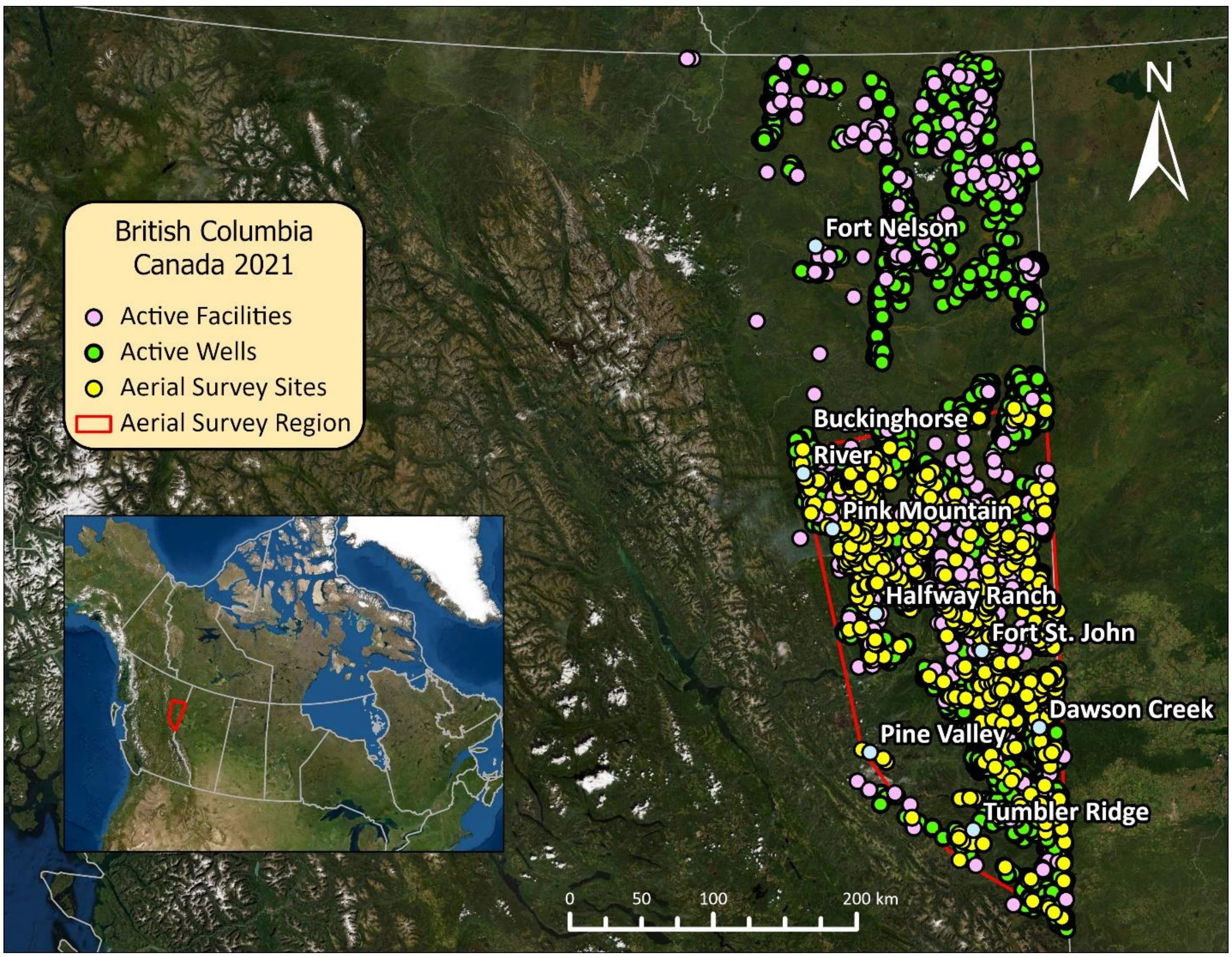

Figure S1: Geographic locations of 508 aerial survey sites in British Columbia, Canada overlaid on the identified locations of 1006 active facilities and 8995 active wells at the time of the survey. The approximately 46,000 km^2 red bounding box is the convex hull of areas of interest (polygons) measured during the present aerial survey. The inset map shows the aerial survey region within the province of BC and Canada.

An initial set of polygons bounding sites for aerial study were manually specified for facility and well locations in this sub-region. These initial polygons were chosen considering the density of sites (to maximize the economics of the survey and the sample size) and the underlying distribution of sites across the sampling strata (to maximize the relative sample size within each stratum). In the final sample, all verifiably active facilities that could be reliably located and had adequate/current satellite imagery within the survey region were included. Initial polygons were provided to Bridger Photonics for flight planning and cost estimation; the remaining budget was leveraged to measure as many well sites within the survey region as feasible. Aerial measurements were ultimately performed over 508 geographically unique sites (polygons) during September 11 to October 8, 2021. Figure S1 maps the geographic distribution of active and measured sites (facilities and wells) during the measurement survey.

As introduced in the manuscript, the developed inventory protocol uses stratified sampling, in which common facility and well types are aggregated into separate strata. Given the complex diversity of methane sources in the UOG industry, parsing sources into strata has some significant benefits supporting the broad objectives of this survey. First, aggregation of like sources tends to reduce the variance of desired statistics describing each sufficiently large stratum; this corresponds to improved precision in a stratum's calculated mean emission rate and total emissions (i.e., emissions inventory). Second, stratification can be used to combine similar but uniquely different entities with limited sample and/or population sizes; this artificial enhancement of sample/population sizes may come at the cost of increased variance but can enable consideration of these entities using robust analytical methods that need sufficiently large sample sizes. Finally, if strata are defined such that each potential source across the province is contained within one and only one stratum (i.e., the strata do not overlap and provide comprehensive coverage), then the provincial emissions inventory is simply the sum of each stratum's inventory. This allows independent analysis of each stratum, permitting stratum-dependent methodologies that may leverage prior information about the strata. Moreover, this approach provides the *relative* contribution of each stratum to the whole, which may be informative for regulatory efforts to mitigate emissions.

Within the Petrinex production data, inventory strata for oil and gas facilities (e.g., batteries, gas gathering systems, gas plants, meter stations, etc.) were naturally defined by existing industry assigned facility subtype codes. For British Columbia there are 53 possible subtypes that group production, process, metering, storage, disposal/waste, and treating facilities into specific categories based on characteristics of the underlying site operations (e.g., single or multi-well batteries, oil or gas production, handling sweet or sour gas, etc.). Active facilities gleaned from the above analysis of monthly production data included 33 unique facility subtypes, which are listed alongside population and sample sizes of the survey in Table S1. Six of these subtypes were combined into two larger categories (meter stations and tank farms) to bolster strata size and simplify analysis; thus, the present inventory analysis considered 29 unique facility-related strata.

Strata for wells considered three well types – gas, oil, and water. Gas well and Oil well strata were derived by combining BCOGC defined wellbore fluid types i) Acid Gas (AGAS), Gas (GAS), and Multiple Gas (MGAS) to Gas; and ii) Oil (OIL), Multiple Oil (MOIL), Multiple Oil and Gas (MOG) to Oil. Wellbore fluid for each surface-hole WA was assigned from the publicly available "Well Surface Hole Locations (Permitted)" file. (BCOGC, 2022c)

Table S1: Summary of facility and off-site well strata in the present aerial survey. Population and sample sizes are shown for 29 facility and three well strata defined for emission inventory development. Excl. = Excluding shut-in facilities/wells; Incl. = Including shut-in facilities/wells.

Facility Description[a]	Facility Type[b]	Combined Type[c]	Well/ Battery Type[d]	Population Size		Sample Size (% of Population)		Entities With Sources (% of Sample)	
				Excl.	*Incl.*	*Excl.*	*Incl.*	*Excl.*	*Incl.*
Gas Transporter	204	—	Other	3	3	1 (33%)	1 (33%)	1 (100%)	1 (100%)
Crude Oil Single-Well Battery	311	—	SWB	52	58	46 (88%)	48 (83%)	5 (11%)	5 (10%)
Crude Oil Multi-Well Group Battery	321	—	MWB	3	5	3 (100%)	3 (60%)	1 (33%)	1 (33%)
Crude Oil Multi-Well Proration Battery	322	—	MWB	35	35	29 (83%)	31 (89%)	12 (41%)	12 (39%)
Gas Single-Well Battery	351	—	SWB	22	28	20 (91%)	21 (75%)	1 (5%)	1 (5%)
Gas Multi-Well Group Battery	361	—	MWB	68	79	50 (74%)	54 (68%)	18 (36%)	18 (33%)
Gas Multi-Well Effluent Measurement Battery	362	—	MWB	135	140	111 (82%)	113 (81%)	55 (50%)	55 (49%)
Mixed Oil and Gas Battery	393	—	MWB	16	16	16 (100%)	16 (100%)	4 (25%)	4 (25%)
Water Hub Battery	395	—	Other	33	34	22 (67%)	22 (65%)	2 (9%)	2 (9%)
Gas Plant Sweet	401	—	MWB	25	25	21 (84%)	21 (84%)	16 (76%)	16 (76%)
Gas Plant; Acid Gas Flaring (<1 t/d Sulphur)	402	—	MWB	22	23	18 (82%)	19 (83%)	14 (78%)	14 (74%)
Gas Plant; Acid Gas Flaring (>1 t/d Sulphur)	403	—	MWB	4	4	2 (50%)	2 (50%)	1 (50%)	1 (50%)
Gas Plant; Acid Gas Injection	404	—	MWB	4	4	3 (75%)	3 (75%)	3 (100%)	3 (100%)
Gas Plant; Sulphur Recovery	405	—	MWB	4	4	3 (75%)	3 (75%)	3 (100%)	3 (100%)
Gas Plant; Fractionation	407	—	MWB	1	1	0	0	—	—
Liquefied Natural Gas (LNG) Plant	451	—	MWB	5	5	1 (20%)	1 (20%)	1 (100%)	1 (100%)
Enhanced Recovery Scheme	501	—	MWB	21	27	17 (81%)	23 (85%)	0	0
Disposal	503	—	Other	57	68	35 (61%)	40 (59%)	2 (6%)	2 (5%)
Acid Gas Disposal	504	—	Other	7	7	6 (86%)	6 (86%)	0	0
Underground Gas Storage	505	—	Other	1	2	1 (100%)	2 (100%)	0	0
Compressor Station	601	—	MWB	254	254	45 (18%)	45 (18%)	25 (56%)	25 (56%)
Custom Treating Facility	611	—	MWB	4	5	4 (100%)	5 (100%)	0	0
Gas Gathering System	621	—	Other	105	139	73 (70%)	92 (66%)	3 (4%)	3 (3%)
Field Receipt Meter Station (MS)	631	MS	Other	91	91	51 (56%)	51 (56%)	5 (10%)	5 (10%)
Interconnect Receipt MS	632								
NEB-Regulated Field Receipt MS	637								
NEB-Regulated Interconnect Receipt MS	638								
Tank Farm (TF); Loading and Unloading Terminal	671	TF	MWB	14	23	9 (64%)	12 (52%)	1 (11%)	1 (8%)
Third Party TF; Loading and Unloading Terminal	673								
Natural Gas Liquids (NGL) Hub Terminal	676	—	MWB	1	1	1 (100%)	1 (100%)	0	0
Surface Waste Facility	701	—	MWB	10	10	8 (80%)	8 (80%)	0	0
Water Source	901	—	SWB	3	3	1 (33%)	1 (33%)	0	0
Water Source Battery	902	—	SWB	6	7	4 (67%)	4 (57%)	0	0
Total:				1006	1101	601 (60%)	648 (59%)	173 (29%)	173 (27%)
Well Bore Fluid			″	″	″	″	″	″	″
Gas[e]			OSW	7772	8629	669 (9%)	744 (9%)	267 (40%)	267 (36%)
Oil[e]			OSW	673	726	28 (4%)	28 (4%)	4 (14%)	4 (14%)
Water			OSW	281	322	5 (2%)	6 (2%)	0	0
Undefined Fluid			OSW	3	3	3 (100%)	3 (100%)	0	0
Total:				8729	9680	705 (8%)	781 (8%)	271 (38%)	271 (35%)

OSW = off site wells; SWB = single well battery; MWB = multi-well battery;

[a] Facility description as per Petrinex database.

[b] 3-digit facility "subtype" used to identify facility type/description in Petrinex.

[c] Combined strata defined as a union of unique facility types.

[d] Strata type for analysis of unmeasured non-pneumatic equipment (see Section S2.2.1).

[e] Excluding shut-in (but including on-site wells), there were 7940 gas, 736 oil, 316 water, and 3 undefined active wellheads. Including shut-in (and including on-site wells) there were 8815 gas, 795 oil, 365 water, and 3 undefined active wellheads at the time of the survey.

S2 Inventory Development

S2.1 Stratum-Level Measured Source Inventories

Beginning with flight pass-level data provided by Bridger, measured emission inventories (within quantified uncertainties) for each stratum were computed in a statistical framework considering measurement quantification accuracy, detection sensitivity, and finite sample size effects. This is possible via the nested algorithms described in this section and summarized at a high-level in Figure 1 of the manuscript.

For each iteration of the analysis, probabilistic average emission rates for each detected and quantified source within each stratum are first computed from pass-by-pass aerial data via the algorithm detailed in Sections S2.1.1 to S2.1.3. Briefly, for each source that is detected one or more times during the aerial survey, Bridger-quantified emission rates are randomly perturbed according to the recently developed quantification error model for Bridger's GML by Conrad et al. (2022). As discussed in Sections S2.1.1 to S2.1.3, it is possible that a source detected during one or more pass of the aircraft may not be detected during one or more of the other passes; this could be due to variability/intermittency of the source and/or the finite detection sensitivity of GML. Given the prior knowledge of an existing source, these "missed detections" are randomly perturbed from zero via a Bayesian analysis according to GML's probability of detection function (Conrad et al., 2022), estimated 3-m wind speed at the time of the flight pass, aircraft altitude, and the quantified emissions data during other flight passes over the source. This provides a randomized, *true* emission rate for each flight pass on each measurement day for the source. Recognizing that variability of the source rate between observations can be expected to increase with the time between observations, a randomized, true, *average* emission rate for the source is obtained by first averaging over all flight passes on each unique measurement day, then averaging over measurement days.

For each facility or well site, the average emission rate(s) of all sources(s) are then summed to yield a randomized, true, total emission rate for that surveyed facility or well pad – which could be zero if no emissions are detected. For aerial survey sites containing only wells, total emissions from shared equipment (e.g., a common separator fed by multiple wells) are equally distributed among the unique wells. Aggregating these facility- and well-level data yields a set of facility/well-level aerial survey emissions (randomly perturbed to consider GML quantification accuracy and detection sensitivity and specifically including measured zeros) for each stratum.

Emissions for sampled sites in each stratum were then scaled to the stratum population to yield the stratum's measured inventory. Except in a few special cases as noted below, this scaling was done using Sitter's mirror-match bootstrap algorithm (Sitter, 1992), which provides a robust probabilistic estimate of the stratum's measured inventory considering the actual (non-smooth, typically skewed) distribution of emissions from sites in the sample as well as finite population effects. The latter is particularly important given that in most cases, the sample represents a significant fraction of the population.

For six strata where the entire populations were sampled (i.e., subtypes 321 – Crude Oil Multi-Well Group Battery, 393 – Mixed Oil and Gas Battery, 505 – Underground Gas Storage, 611 – Custom Treating Facility, 676 – Natural Gas Liquids Hub Terminal, and wells of undefined fluid; see Table S1), the measured inventory was directly quantified and no further scaling was required. Similarly, for six strata where no emissions were detected (i.e., subtypes 501 - Enhanced Recovery Scheme, 504 - Acid Gas Disposal, 701 - Surface Waste Facility, 901 - Water Source, 902 – Water Source Battery, and water wells; see Table S1) the measured inventory was conservatively assumed to be zero despite the potential for emitters at entities that were not surveyed. For three subtypes (204 – Gas Transporter, 403 – Gas Plant with Acid Gas Flaring (> 1 t/d Sulphur), and 451 – Liquefied Natural Gas Plant; see Table S1) with small populations (3–5 facilities) and only one facility each with detected emissions, the measured inventory was assumed to probabilistically follow a uniform distribution bounded by two simple cases: a) all unsurveyed entities had zero emissions and b) all unsurveyed entities had emissions equal to the single surveyed entity. Lastly, for a single facility subtype (407 – Gas Plant; Fractionation) that was not surveyed, emissions were estimated by computing the population size-weighted average of facility-level emissions for 47 other gas plants (subtypes 401-405).

Finally, the measured inventory for the province was computed by summing the measured inventories of the 33 unique strata. To fully resolve the effects of GML's quantification error and detection sensitivity, flight pass-level emissions were randomly perturbed as described above $B_{\mathrm{MC}} = 10^4$ times (where the subscript "MC" represents the Monte Carlo considering effects related to the performance of the GML technology). For each of the B_{MC} sets of randomly perturbed flight pass-level emissions, the measured inventory of each stratum and, hence, the province was computed $B_{\mathrm{BS}} = 10^4$ times (where "BS" implies that this analysis considers effects related to sample sizes via the bootstrapping or alternate approaches noted above). Ultimately, this provided $B_{\mathrm{MC}} \times B_{\mathrm{BS}} = 10^8$ estimates of the provincial measured inventory for which statistics could be obtained. Final measured provincial and stratum inventory statistics are summarized in Table S4 and Table S5. Reference mean population emission factors for each facility and well stratum would be obtainable by dividing each stratum inventory by the corresponding population from Table S1.

S2.1.1 Successfully Detected Emissions

During the aerial survey, all sites with detected sources were re-flown at least once, 1–10 days after the initial flight, where each flight contained up to 5 passes over each source. Given finite detection sensitivities coupled with the potential for source variability and intermittency, it is possible that any source may be detected and quantified during some flight passes but missed during others. When a source is successfully detected, a randomized true value of the instantaneous emission rate for that flight pass can be computed from the measured emission rate using a quantification error model for Bridger's GML.

Recently, Conrad et al. (2022) analyzed data from fully and semi-blinded controlled release experiments to derive a quantification error model for Bridger's GML technology. The error model defines the probability of the true source emission rate (Q) given Bridger's estimate ($\tilde{Q}$) for each measurement pass of the airplane; the error model is in the form of a conditional probability distribution denoted by $\pi(Q|\tilde{Q})$. The inverse cumulative distribution function of $\pi(Q|\tilde{Q})$ provides an efficient means to randomly draw a true pass-level emission rate from Bridger's estimated value. From Table S3 of Conrad et al. (2022):

$$Q = \alpha d(\xi^{-1} - 1)^{-1/\beta}\tilde{Q} \tag{S1}$$

where the unitless coefficients α, β, and d are 0.891, 3.82, and 0.918, respectively, and ξ is a randomly drawn number from the standard uniform distribution.

S2.1.2 Bayesian Analysis of Sources with "Missed" Detections During One or More Passes

For any detected methane source, the pass-by-pass aerial measurement data may include one or more passes in which the source was not detected ("missed"). This may be due to the probabilistic nature of detection success by the airplane, finite detection sensitivities for the GML technology, source variability considering these first two factors, or source intermittency. This section describes a robust Bayesian approach to analyze sources that have been both quantified and "missed" during different measurement passes. The method derives a probability distribution for the *true* emission rate of a known source that is missed during an individual pass, leveraging pass-specific POD data (based on airplane altitude and wind speed for each pass) as well as quantified source rate(s) from all other passes.

Let $\tilde{Q}$ and Q represent the Bridger-estimated and true source rate and $\tilde{u}$ and u represent the Bridger-estimated and (unknown) true 3-m wind speed during a flight pass. Similarly let $\tilde{h}$ represent the aircraft altitude above ground level during the pass. Finally, define a unitless binary variable D to signify a successful detection ($D = 1$) or a missed detection ($D = 0$; denoted as $\neg D$, "not D"). With these definitions, the objective is to derive the conditional probability distribution:

$$\pi\left(Q \middle| \tilde{u}, \tilde{h}, \neg D\right) \tag{S2}$$

That is, the probability of the source's true instantaneous emission rate conditional on the Bridger-estimated 3-m wind speed and aircraft altitude for the missed detection.

Using the Bayesian perspective, which treats all variables as probabilistic random variates, the conditional probability of Eq. (S2) is proportional to the joint distribution of all variables:

$$\pi\left(Q \middle| \tilde{u}, \tilde{h}, \neg D\right) \propto \pi\left(Q, \tilde{u}, \tilde{h}, \neg D\right) \tag{S3}$$

The righthand side of Eq. (S3) can be re-stated as

$$\pi\left(Q \middle| \tilde{u}, \tilde{h}, \neg D\right) \propto \int_0^\infty \pi\left(Q, \tilde{u}, u, \tilde{h}, \neg D\right) du \tag{S4}$$

by introducing the true 3-m wind speed to the joint distribution and subsequently marginalizing it out via integration over the positive real numbers. By assuming that the true source rate and wind speed are statistically independent and the uncertainty on aircraft altitude is negligible, the chain rule can be used to expand the joint distribution in Eq. (S4) to give

$$\pi\left(Q\middle|\tilde{u},\tilde{h},\neg D\right) \propto \int_0^\infty \pi\left(\neg D\middle|Q,u,\tilde{h}\right)\pi(u|\tilde{u})\pi_{pri}(Q)du \tag{S5}$$

where $\pi(u|\tilde{u})$ is a probabilistic error model for the 3-m wind speed (i.e., the conditional probability of the true 3-m wind speed given the Bridger-estimated 3-m wind speed) and $\pi_{pri}(Q)$ represents a prior distribution for the true emission rate of the source. The conditional probability $\pi\left(\neg D\middle|Q,u,\tilde{h}\right)$ is the likelihood of a missed detection given a true emission rate, 3-m wind speed, and aircraft altitude; this is the complement of the probability of detection function (POD)

$$\pi\left(Q\middle|\tilde{u},\tilde{h},\neg D\right) \propto \int_0^\infty \left(1 - POD\left(Q,u,\tilde{h}\right)\right)\pi(u|\tilde{u})\pi_{pri}(Q)du \tag{S6}$$

As is typical in Bayesian analyses, the normalizing constant of proportionality (necessary to satisfy the law of total probability) can be obtained by integrating the righthand side of Eq. (S6) over Q such that

$$\pi\left(Q\middle|\tilde{u},\tilde{h},\neg D\right) = \frac{\int_0^\infty \left(1 - POD\left(Q,u,\tilde{h}\right)\right)\pi(u|\tilde{u})\pi_{pri}(Q)du}{\int_0^\infty \int_0^\infty \left(1 - POD\left(Q,u,\tilde{h}\right)\right)\pi(u|\tilde{u})\pi_{pri}(Q)du\,dQ} \tag{S7}$$

Two of three elements on the righthand side of Eq. (S7), the probability of detection function $\left(POD\left(Q,u,\tilde{h}\right)\right)$ and the error model for the 3-m wind speed $\left(\pi(u|\tilde{u})\right)$, are available in the literature (Conrad et al., 2022). Thus, the presented analysis only requires a choice of prior distribution for the true source rate. Theoretically an “uninformed”/non-negative prior, which fixes $\pi_{pri}(Q)$ to a constant value for all positive values of Q could be used. However, this is overly simplistic since it ignores measurement data from other passes where the same source was detected and quantified. Additionally, the “uninformed” prior does not impose an upper-bound on a missed detection rate. To address this latter point, in the present work missed detection rates are upper bounded by the largest measured emission rate for that source during the measurement survey. Thus, by defining $\pi_{pri}(Q)$ as the uniform distribution from 0 to $\hat{Q}$, where $\hat{Q}$ is the largest detected and quantified true emission rate of the source (obtained from data calculated using Eq. (S1)), Eq. (S7) simplifies to

$$\pi\left(Q\middle|\tilde{u},\tilde{h},\neg D\right)=\frac{\int_0^{\infty}\left(1-POD\left(Q,u,\tilde{h}\right)\right)\pi(u|\tilde{u})du}{\int_0^{\hat{Q}}\int_0^{\infty}\left(1-POD\left(Q,u,\tilde{h}\right)\right)\pi(u|\tilde{u})du\,dQ} \tag{S8}$$

Finally, as in Section S2.1.1, if ξ is a randomly drawn number from the standard uniform distribution, then a randomized value of the emission rate during a missed detection given an estimated 3-m wind speed and aircraft altitude can be obtained by integrating the conditional distribution of Eq. (S8) and solving for Q:

$$Q:\xi=\frac{\int_0^{Q}\int_0^{\infty}\left(1-POD\left(Q',u,\tilde{h}\right)\right)\pi(u|\tilde{u})du\,dQ'}{\int_0^{\hat{Q}}\int_0^{\infty}\left(1-POD\left(Q',u,\tilde{h}\right)\right)\pi(u|\tilde{u})du\,dQ'} \tag{S9}$$

which, for the published forms of the probability of detection function and wind speed error model, requires numerical integration and root-finding methods.

S2.1.3 Procedure for Averaging Source Measurements During Different Passes and Flights

Flight pass-level emission rates for each source are averaged as described by Tyner and Johnson (2021) after randomization of flight pass level emission rates as described above. Firstly, randomized flight pass-level emission rates are averaged over each measurement date and these are then averaged over the measurement dates in the survey. Let Q_{mn} be the *randomized* true emission rate during the n^{th} flight pass on the m^{th} measurement date. Furthermore, define M as the total number of measurement dates and N_m as the total number of flight passes on the m^{th} measurement day for which the source lies within the GML sensor's field of view. With these definitions, a randomized, true, average source rate during the measurement campaign ($\bar{Q}$) for the source is:

$$\bar{Q} = \frac{1}{M}\sum_{m=1}^{M}\frac{1}{N_m}\sum_{n=1}^{N_m} Q_{mn} \tag{S10}$$

S2.2 Unmeasured Sources – Site-Level Emission Factor Development

As detailed in the main text, unmeasured sources are those that are not detected during *any* flight pass of the measurement survey. Depending on the underlying source distribution, measurement conditions, and sensitivity of the aerial measurement technology, these sources can represent a significant portion of the total inventory and must be considered. The present methodology calculates the unmeasured inventory by combining site counts with site-level emission factors that are estimated via a Monte Carlo (MC) simulation of aerial survey over sources near and below the aerial technology's sensitivity limit. This procedure is summarized in Figure 1b of the main text and detailed in this section.

Given the inherent lack of emission rate data for sources not detected aerially, the first requirement for this analysis is a representative feedstock dataset that provides a source rate distribution near and below the aerial technology's sensitivity limit. In the current work, high-sensitivity measurement data of site/stratum- and source-resolved emissions were available from a 2018 ground survey in British Columbia of 267 facilities and wells (Robinson et al., 2018). These data include quantified emissions from non-pneumatic equipment and abnormally operating pneumatic equipment detected by optical gas imaging and measured where possible using Hi-Flow sampling. Robinson et al. (2018) also counted and identified (manufacturer and model) pneumatic equipment and estimated expected emissions under normal operation based on prior field measurements and manufacturer-specific bleed rates.

To accurately infer the unmeasured inventory, the simulated aerial survey of the feedstock data must be performed similarly to the actual survey. Recalling that unmeasured sources are defined as *never* being detected during the potentially many flight passes over the source, it is imperative to simulate an appropriate number of flight passes and assume representative measurement conditions, which inform the probability of detecting any one source during a single pass. To this end, for the present study, an empirical probability mass function (PMF) of the number of flight passes over a source was obtained from the aerial survey data (see Figure S2a). Likewise, recognizing that the best-available continuous probability of detection (POD) function for Bridger's GML technology is sensitive to the estimated local wind speed ($\tilde{u}$ [m/s]; at 3 m elevation) and aircraft altitude above ground level (AGL; $\tilde{h}$ [m]) (Conrad et al., 2022), empirical probability density functions (PDFs) for these parameters were similarly derived from flight pass-level data during the aerial survey and are shown in Figure S2b and c, respectively. For a single steady methane source, these distributions enable representative simulation of the probability that the source would be detected during a multi-pass aerial survey using Bridger's GML.

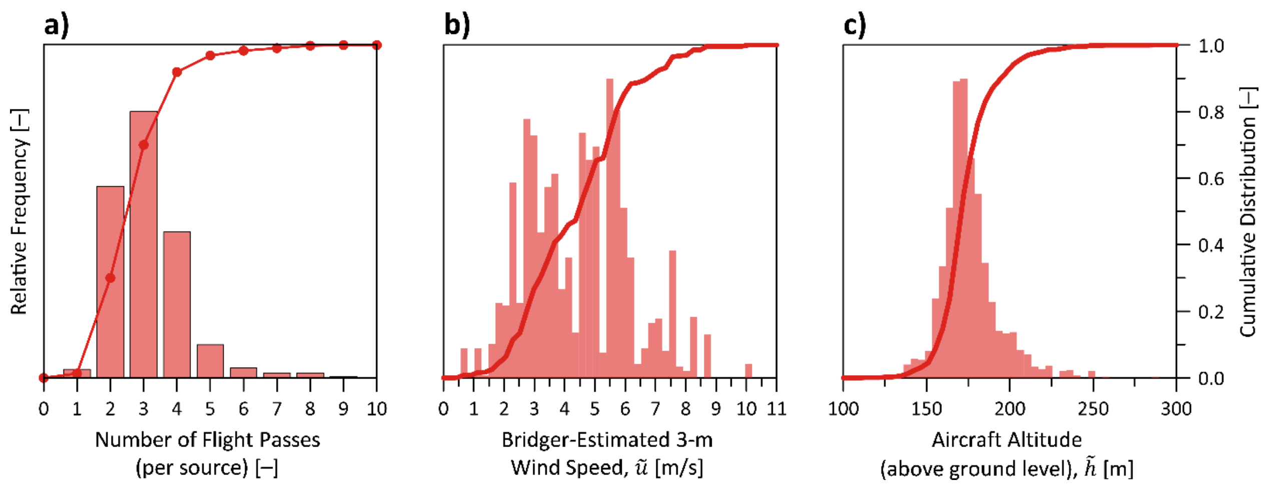

Figure S2: Empirical probability mass (a) and density (b, c) functions for the number of flight passes per source (a), estimated 3-m wind speed (b; $\tilde{u}$), and aircraft altitude (c; $\tilde{h}$).

S2.2.1 Non-pneumatic Equipment

With the feedstock data, empirical PMF for number of flight passes (see Figure S2a), empirical PDFs for measurement conditions (see Figure S2b and c), and the continuous POD function for the aerial technology, the MC simulation can proceed. Consider an example MC simulation of a specific equipment type (here, non-pneumatic equipment) within a single stratum and refer to the flowchart of the MC procedure shown in Figure S3. Let the index $l \in \{1, \cdots, L\}$ represent the relevant sources in the feedstock data and let $\tilde{Q}_l$ represent the corresponding estimated source rate. Denote the total number of relevant ground-surveyed sites as K.

Each b of B_{MC} total MC iterations begins by initializing the *total* unmeasured emissions within the stratum to zero $\left(Q_{[b]} = 0\right)$. The simulation proceeds by considering the first detected source ($l = 1$). A randomized number of flight passes (N) is obtained by random sampling of the empirical PMF. For each $n \in \{1, \cdots, N\}$ flight pass, a random estimated 3-m wind speed ($\tilde{u}$) and aircraft altitude (h) is obtained from the respective empirical PDF. These are combined with the source rate ($\tilde{Q}_l$) through Eq. (10) of Conrad et al. (2022) to yield the probability of detecting the source during that single flight pass $\left(POD\left(\tilde{Q}_l, \tilde{u}, h\right)\right)$. If the POD exceeds a random number (ξ) drawn from the standard uniform distribution, then the source is *detected/measured* and the source does not contribute to the unmeasured inventory; the simulation moves to the next source ($l \leftarrow l + 1$) without further action. Alternatively, if $\xi > POD\left(\tilde{Q}_l, \tilde{u}, h\right)$, the source is *missed/unmeasured* during the n^{th} flight pass and the next flight pass is simulated by drawing a new $\tilde{u}$, h, and ξ and repeating the process. If the source is missed during all N flight passes, then it contributes to the unmeasured inventory and the total unmeasured emissions are updated $\left(Q_{[b]} \leftarrow Q_{[b]} + \tilde{Q}_l\right)$.

After iterating through all L sources, $Q_{[b]}$ contains the MC-simulated total unmeasured emissions for the equipment type and stratum. This is divided by the total number of ground-surveyed sites (K) to give one MC-simulated, site-averaged emission factor $\left(\bar{Q}_{[b]} = Q_{[b]}/K\right)$ for the equipment type and stratum, which marks the end of the MC iteration. After B_{MC} (10^5 in this study) iterations, the mean of the MC estimates is taken as the average site-level emission factor for unmeasured sources of the specific equipment type in the stratum – i.e., $\bar{Q} = \sum_b \bar{Q}_{[b]} / B_{\text{MC}}$.

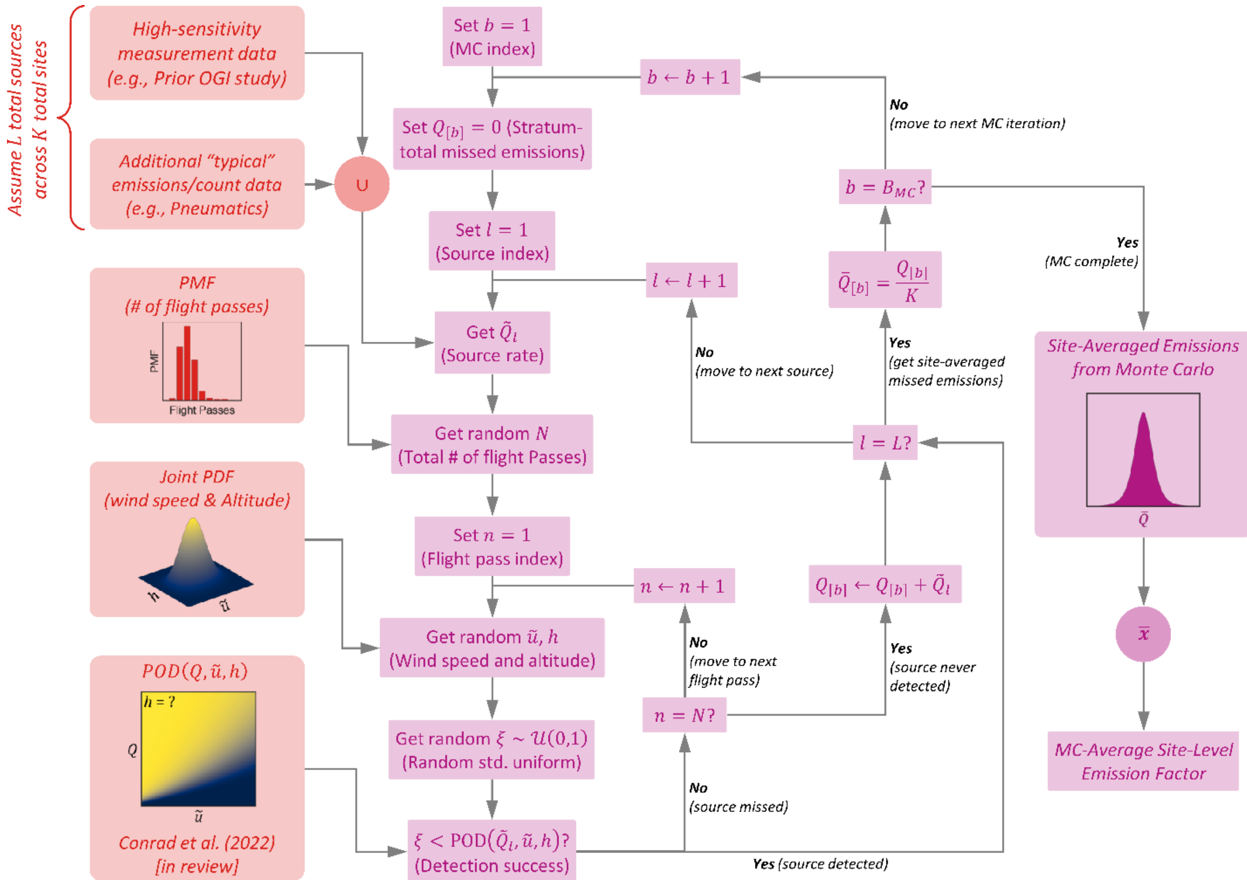

Figure S3: Monte Carlo analysis procedure for quantifying unmeasured sources (i.e., sources that are not detected during any pass of the aerial survey).

Non-pneumatic sources in the feedstock data were parsed into four facility/well categories prior to analysis using the presented method. Each stratum in the provincial inventory (refer to Table S1) was captured by one of these categories: off-site wells (OSW), single-well batteries (SWB; facilities with one linked well), multi-well batteries (MWB; facilities with multiple linked wells), and other (facilities with no associated wells). Strata in the "other" category had no feedstock data and were conservatively assumed to have zero unmeasured non-pneumatic emissions. Average site-level emission factors for the OSW, SWB, and MWB categories were computed using the described methodology and are summarized in Table S2.

Table S2: Derived emission factors for unmeasured methane sources.

Category	Assigned Strata	Average Site-Level Emission Factor [kg/h/facility or well]
Off-Site Wells (OSW)	Well types of all bore fluids (gas, oil, water, undefined)	0.069
Single-Well Batteries (SWB)	Facility types 311, 351, 901, and 902	0.213
Multi-Well Batteries (MWB)	Facility types 321, 322, 361, 362, 393, 401, 402, 403, 404, 405, 407, 451, 501, 601, 611, 676, and 701 and tank farms	0.383
Other	Facility types 204, 395, 503, 504, 505, 621, and meter stations	0[a]

[a] Unmeasured, non-pneumatic emissions assumed to be zero.

S2.2.2 Pneumatic Equipment

Pneumatic instruments (e.g., level controllers, pressure controllers, transducers, positioners, etc.) and pumps are ubiquitous in process equipment buildings (e.g., separators, line heaters, compressor buildings, etc.) across production sites in the upstream oil and gas sector. In bottom-up component-based inventories, pneumatic emissions are generally estimated by multiplying average device emission factors by the corresponding device counts aggerated over well and facility population strata (Clearstone Engineering Ltd., 2018; Robinson et al., 2018). In the present inventory, average site-level emission factors for pneumatic equipment were derived using the same method described for unmeasured non-pneumatics (see Section S2.2.1). For pneumatic equipment, however, this approach simplifies the method of Figure S3 because normally operating pneumatic devices generally vent at sufficiently low rates to preclude detection by aerial technologies; this is supported by the present aerial survey and follow-up ground survey (Johnson et al., 2022). Firstly, average vent rates for the pneumatic instruments and pumps in BC derived by (Robinson et al., 2018) using data from (AER, 2018; D'Antoni, 2018; Government of Alberta, 2020; Prasino Group, 2013; Western Climate Initiative, 2013) were less than 0.4 and 0.6 kg/h of methane, respectively, which correspond to a negligible POD even when using Bridger's highly sensitive GML technology. Indeed, at the median wind speed and typical aircraft altitude of the survey (4.5 m/s and 175 m AGL, respectively), the predicted single-pass PODs at these rates are less than 10^{-5}. This low POD is evidenced by the present survey data itself, where methane was not detected using Bridger's GML at 603 active surveyed sites (177 facilities and 426 off-site wells) where pneumatic equipment would be expected. Moreover, follow-up ground survey of

195 aerially detected sources at 75 locations (Johnson et al., 2022) implicated pneumatic instruments and pumps as a *potential* contributor to just 24 sources. However, make and model data from pneumatic devices suggest that, if pneumatics were the cause of these 24 aerially detected sources, the identified pneumatics would need to be emitting approximately an order of magnitude greater than published/manufacturer-rated vent rates. However, this is also unlikely given the field data from the 2018 ground survey in BC (Robinson et al., 2018), where pneumatics deemed to be operating abnormally emitted at rates near the published/manufacturer-rated vent rates. These observations permit the reasonable assumption that normally operating pneumatics were not detected during the present aerial survey using Bridger Photonics GML.

Since probabilistic detection of normally operating pneumatic sources can justifiably be ignored, average site-level unmeasured pneumatic emission factors were derived using the same methodology as unmeasured non-pneumatic equipment (Section S2.2.1 and Figure S3). This procedure is thus greatly simplified as it does not require MC analysis of detection sensitivity; all pneumatic equipment contribute to the site-level emission factor, which is simply the average site-total vent rate of pneumatic equipment. In this case, the contribution of unmeasured pneumatic equipment to the provincial inventory reduces to the classic bottom-up approach that combines individual pneumatic counts and typical vent rates (emission factors) to yield site-level emissions. It should be noted that this calculation is likely conservatively low, since the preceding discussion also suggests abnormally operating pneumatics (at least at the magnitudes observed in the field measurements of Robinson et al. (2018) are likely missed by the aerial survey and are excluded in this bottom-up estimate.

Measurement-based, average emission factors were derived by Robinson et al. (2018) from pneumatic counts of individual makes and models, collected during the 2018 ground-based OGI survey of production sites in BC, and combined with measured venting data from pneumatic studies in BC and Alberta (AER, 2018; D'Antoni, 2018; Government of Alberta, 2020; Prasino Group, 2013; Western Climate Initiative, 2013). Strata-specific average emission factors for pneumatic equipment are summarized in Table S3; emission factors for well strata are on a per-wellhead basis and applied to all surface wells in the province (see Table S1, footnote e) while emission factors for facility strata are on a per-site basis. Originally reported in units of m^3/h of natural gas in Table 15 of Robinson et al. (2018), these were converted to kg/h of methane assuming a methane content of 88% by volume and a methane density of 0.6785 kg/m^3 at standard conditions (1 atm and 15°C). For gas well and gas facility strata, venting rates reported for conventional and tight gas production types were averaged and weighted by site type. Finally, a venting rate for mixed oil and gas batteries – multi-well facilities that report both gas and oil production – was estimated using the weighted average of all oil and gas multi-well batteries. As in Tyner and Johnson (2021) emissions from pneumatics at facility strata not covered by the 2018 OGI survey (e.g., gas plants, custom treaters, LNG Plant, custom treaters, etc.) were conservatively assumed to be zero under the assumption that pneumatics at the majority of these larger facilities are instrument air-driven. Likewise, methane emissions from pneumatic chemical injection pumps were estimated using a seasonal operation factor of 50%, an average vent rate of 0.973 m^3 gas/h (Clearstone Engineering Ltd., 2018) – corresponding to 0.5807 kg/h of methane at the standard conditions noted above and again assuming a methane content of 88% by volume – and mean chemical injection pump counts for well and facility strata derived from the 2018 OGI survey, weighted by site type, for natural gas driven pumps (Robinson et al., 2018, Table 16). Consistent with pneumatic instrument emission factor estimates, the mean number of chemical injection pumps at mixed oil and gas batteries were estimated by averaging pump counts across all oil and gas multi-well battery strata weighted by site type. A seasonal operation factor of 50%, based on an assumed six months of operation per year consistent with the national inventory, discounts the contribution of pneumatic pumps to the unmeasured inventory as it inherently ignores pumps that may operate throughout the year. Importantly, this seasonal operation discount factor is likely to underestimate annual-averaged pneumatic pump emissions as some implementations are designed to operate more frequently – e.g., corrosion inhibitor pumps effectively operate constantly.

Table S3: Average site-level emission factors for pneumatic equipment and relevant strata. Emission factors are in units of vent rate [kg/h] per entity, where "entity" corresponds to "wellheads" for the Gas/Oil Well rows and "sites" otherwise.

Facility/Well Description	Facility Type	Pneumatic Devices	Pneumatic Pumps		Total
		Average EF [kg/h/entity]	*Average EF [kg/h/entity]*	*Seasonal Operation*	*Average EF [kg/h/entity]*
Gas Well	—	0.190	0.270	×0.5	0.325
Oil Well	—	0.131	0.110	×0.5	0.187
Crude Oil Single-Well Battery	311	0.239	0.412	×0.5	0.445
Crude Oil Multi-Well Group Battery	321	0.179	0.726	×0.5	0.542
Crude Oil Multi-Well Proration Battery	322	0.382	—	—	0.382
Gas Single-Well Battery	351	0.156	0.499	×0.5	0.405
Gas Multi-Well Group Battery	361	0.142	0.548	×0.5	0.416
Gas Multi-Well Effluent Measurement Battery	362	0.181	0.216	×0.5	0.289
Mixed Oil and Gas Battery	393	0.197	0.347	×0.5	0.370

S2.3 Inventory Summary

Table S4: British Columbia 2021 upstream oil and gas methane inventory excluding "shut-in" facilities.

Strata Description	Facility/Combined Type or Well Bore Fluid	Measured Inventory [kt/y]	Unmeasured Inventory [kt/y]			Total Inventory [kt/y]
			Non-pneumatic Equipment	*Pneumatic Instruments*	*Pneumatic Pumps*	
Gas Transporter	204	0.82 (0.10, 1.60)	0	0	0	0.82 (0.10, 1.60)
Crude Oil Single-Well Battery	311	0.16 (0.09, 0.24)	0.10	0.11	0.09	0.46 (0.39, 0.54)
Crude Oil Multi-Well Group Battery	321	0.02 (0.01, 0.05)	0.01	0.00	0.01	0.05 (0.03, 0.08)
Crude Oil Multi-Well Proration Battery	322	0.78 (0.44, 1.17)	0.12	0.12	0	1.02 (0.67, 1.41)
Gas Single-Well Battery	351	0.19 (0, 0.37)	0.04	0.03	0.05	0.31 (0.12, 0.49)
Gas Multi-Well Group Battery	361	4.63 (2.47, 6.97)	0.23	0.08	0.16	5.11 (2.94, 7.45)
Gas Multi-Well Effluent Measurement Battery	362	14.50 (11.23, 17.09)	0.45	0.21	0.13	15.29 (12.02, 17.88)
Mixed Oil and Gas Battery	393	0.40 (0.29, 0.57)	0.05	0.03	0.02	0.51 (0.40, 0.67)
Water Hub Battery	395	0.04 (0, 0.09)	0	0	0	0.04 (0, 0.09)
Gas Plant Sweet	401	17.18 (12.02, 22.39)	0.08	0	0	17.27 (12.11, 22.48)
Gas Plant; Acid Gas Flaring (<1 t/d Sulphur)	402	3.93 (2.56, 5.08)	0.07	0	0	4.00 (2.64, 5.16)
Gas Plant; Acid Gas Flaring (>1 t/d Sulphur)	403	2.11 (0.26, 3.71)	0.01	0	0	2.12 (0.28, 3.72)
Gas Plant; Acid Gas Injection	404	1.74 (1.22, 2.69)	0.01	0	0	1.75 (1.23, 2.71)
Gas Plant; Sulphur Recovery	405	1.56 (1.05, 2.31)	0.01	0	0	1.58 (1.07, 2.32)
Gas Plant; Fractionation	407	0.45 (0.35, 0.55)	0.00	0	0	0.45 (0.36, 0.55)
LNG Plant	451	1.03 (0.12, 2.21)	0.02	0	0	1.05 (0.14, 2.23)
Enhanced Recovery Scheme	501	0	0.07	0	0	0.07
Disposal	503	0.45 (0, 0.94)	0	0	0	0.45 (0, 0.94)
Acid Gas Disposal	504	0	0	0	0	0
Underground Gas Storage	505	0	0	0	0	0
Compressor Station	601	45.72 (27.03, 67.96)	0.85	0	0	46.57 (27.88, 68.81)
Custom Treating Facility	611	0	0.01	0	0	0.01
Gas Gathering System	621	0.73 (0.06, 1.36)	0	0	0	0.73 (0.06, 1.36)
Meter Stations	MS	0.16 (0.05, 0.30)	0	0	0	0.16 (0.05, 0.30)
Tank Farms	TF	0.03 (0, 0.08)	0.05	0	0	0.07 (0.05, 0.12)
NGL Hub Terminal	676	0	0.00	0	0	0.00
Surface Waste Facility	701	0	0.03	0	0	0.03
Water Source	901	0	0.01	0	0	0.01
Water Source Battery	902	0	0.01	0	0	0.01
Wells	Gas	14.83 (11.24, 19.67)	4.70	13.21	9.40	42.14 (38.54, 46.98)
Wells	Oil	0.73 (0.14, 1.76)	0.41	0.85	0.36	2.34 (1.75, 3.37)
Wells	Water	0	0.17	0	0	0.17
Wells	Undefined	0	0.002	0	0	0.00
	Total:	112.2 (91.7, 135.9)	7.54	14.64	10.23	144.6 (124.1, 168.3)

Table S5: British Columbia 2021 upstream oil and gas methane inventory including "shut-in" facilities.

Strata Description	Facility/Combined Type or Well Bore Fluid	Measured Inventory [kt/y]	Unmeasured Inventory [kt/y]			Total Inventory [kt/y]
			Non-pneumatic Equipment	*Pneumatic Instruments*	*Pneumatic Pumps*	
Gas Transporter	204	0.82 (0.10, 1.60)	0	0	0	0.82 (0.10, 1.60)
Crude Oil Single-Well Battery	311	0.17 (0.08, 0.27)	0.11	0.12	0.10	0.50 (0.42, 0.60)
Crude Oil Multi-Well Group Battery	321	0.04 (0, 0.13)	0.02	0.01	0.02	0.08 (0.04, 0.17)
Crude Oil Multi-Well Proration Battery	322	0.73 (0.44, 1.07)	0.12	0.12	0	0.97 (0.67, 1.31)
Gas Single-Well Battery	351	0.23 (0, 0.52)	0.05	0.04	0.06	0.39 (0.15, 0.67)
Gas Multi-Well Group Battery	361	4.98 (2.54, 7.72)	0.27	0.10	0.19	5.53 (3.09, 8.27)
Gas Multi-Well Effluent Measurement Battery	362	14.76 (11.37, 17.50)	0.47	0.22	0.13	15.59 (12.19, 18.32)
Mixed Oil and Gas Battery	393	0.40 (0.29, 0.57)	0.05	0.03	0.02	0.51 (0.40, 0.67)
Water Hub Battery	395	0.04 (0, 0.10)	0	0	0	0.04 (0, 0.10)
Gas Plant Sweet	401	17.18 (12.02, 22.40)	0.08	0	0	17.27 (12.10, 22.48)
Gas Plant; Acid Gas Flaring (<1 t/d Sulphur)	402	3.89 (2.54, 5.01)	0.08	0	0	3.97 (2.61, 5.09)
Gas Plant; Acid Gas Flaring (>1 t/d Sulphur)	403	2.11 (0.26, 3.71)	0.01	0	0	2.12 (0.28, 3.72)
Gas Plant; Acid Gas Injection	404	1.74 (1.22, 2.69)	0.01	0	0	1.75 (1.23, 2.71)
Gas Plant; Sulphur Recovery	405	1.56 (1.05, 2.31)	0.01	0	0	1.58 (1.07, 2.32)
Gas Plant; Fractionation	407	0.44 (0.35, 0.54)	0.00	0	0	0.44 (0.35, 0.54)
LNG Plant	451	1.03 (0.12, 2.21)	0.02	0	0	1.05 (0.14, 2.23)
Enhanced Recovery Scheme	501	0	0.09	0	0	0.09
Disposal	503	0.47 (0, 1.01)	0	0	0	0.47 (0, 1.01)
Acid Gas Disposal	504	0	0	0	0	0
Underground Gas Storage	505	0	0	0	0	0
Compressor Station	601	45.72 (27.03, 67.97)	0.85	0	0	46.57 (27.89, 68.82)
Custom Treating Facility	611	0	0.02	0	0	0.02
Gas Gathering System	621	0.76 (0.05, 1.47)	0	0	0	0.76 (0.05, 1.47)
Meter Stations	MS	0.16 (0.05, 0.30)	0	0	0	0.16 (0.05, 0.30)
Tank Farms	TF	0.03 (0, 0.11)	0.08	0	0	0.11 (0.08, 0.19)
NGL Hub Terminal	676	0	0.00	0	0	0.00
Surface Waste Facility	701	0	0.03	0	0	0.03
Water Source	901	0	0.01	0	0	0.01
Water Source Battery	902	0	0.01	0	0	0.01
Wells	Gas	14.81 (11.20, 19.65)	5.22	14.66	10.44	45.13 (41.52, 49.97)
Wells	Oil	0.79 (0.15, 1.90)	0.44	0.92	0.38	2.53 (1.89, 3.64)
Wells	Water	0	0.19	0	0	0.19
Wells	Undefined	0	0.002	0	0	0.00
	Total:	112.9 (92.3, 136.7)	8.26	16.21	11.35	148.7 (128.1, 172.5)

Table S6: British Columbia 2021 upstream oil and gas methane inventory by stratum and source (derived for the case excluding "shut-in" facilities).

Strata Description	Facility/ Combined Type or Well Bore Fluid	Sources														Total
		Compressor Buildings	*Dehydrators*	*Flares (Lit)*	*Flares (Unlit)*	*Line Heater*	*Other*	*Piping*	*Power Generators*	*Separators*	*Tanks*	*Wellhead*	*Unknown*	*Pneumatic Instruments*	*Pneumatic Pumps*	
Gas Transporter	204	0	0	0	0	0	0	0	0	0	0	0	0.817	0	0	0.817
Crude Oil Single-Well Battery	311	0.053	0.009	0	0	0.002	0	0.024	0	0.089	0.072	0.006	0	0.109	0.094	0.458
Crude Oil Multi-Well Group Battery	321	0.005	0.001	0	0.024	0.000	0.000	0.000	0.000	0.002	0.002	0.000	0	0.005	0.010	0.048
Crude Oil Multi-Well Proration Battery	322	0.110	0.079	0	0.291	0.000	0.004	0.005	0.001	0.035	0.373	0.003	0	0.117	0	1.018
Gas Single-Well Battery	351	0.006	0.054	0	0	0.001	0	0.010	0	0.014	0.147	0.003	0	0.030	0.048	0.313
Gas Multi-Well Group Battery	361	1.337	0.246	0	1.874	0.036	0.320	0.057	0.002	0.261	0.693	0.005	0.026	0.085	0.163	5.107
Gas Multi-Well Effluent Measurement Battery	362	10.56	1.046	0	0.222	0.018	0.097	0.034	0.365	0.711	1.501	0.011	0.384	0.214	0.128	15.29
Mixed Oil and Gas Battery	393	0.276	0.085	0	0	0.000	0.002	0.002	0.001	0.011	0.076	0.001	0	0.028	0.024	0.506
Water Hub Battery	395	0	0	0	0	0	0	0	0	0	0.016	0	0.022	0	0	0.038
Gas Plant Sweet	401	10.27	0.155	0	0.767	0.240	0.033	0.241	0.771	0.039	4.524	0.002	0.227	0	0	17.27
Gas Plant; Acid Gas Flaring (<1 t/d Sulphur)	402	2.049	0.113	0.038	0.094	0.034	0.235	0.097	0.606	0.046	0.584	0.002	0.105	0	0	4.002
Gas Plant; Acid Gas Flaring (>1 t/d Sulphur)	403	1.485	0.001	0	0	0.000	0.175	0.001	0.000	0.003	0.456	0.000	0	0	0	2.121
Gas Plant; Acid Gas Injection	404	0.363	0.001	0	0	0.000	0.000	0.001	0.815	0.003	0.500	0.000	0.066	0	0	1.748
Gas Plant; Sulphur Recovery	405	0.631	0.001	0.042	0	0.000	0.000	0.001	0.000	0.003	0.338	0.000	0.561	0	0	1.577
Gas Plant; Fractionation	407	0.241	0.006	0.002	0.013	0.004	0.013	0.007	0.049	0.002	0.097	0.000	0.019	0	0	0.453
LNG Plant	451	0.972	0.001	0	0	0.000	0.069	0.001	0.000	0.003	0.003	0.000	0	0	0	1.049
Enhanced Recovery Scheme	501	0.032	0.005	0	0	0.000	0.002	0.003	0.001	0.014	0.011	0.002	0	0	0	0.070
Disposal	503	0	0.085	0	0.124	0	0.043	0	0	0	0.054	0	0.142	0	0	0.448
Acid Gas Disposal	504	0	0	0	0	0	0	0	0	0	0	0	0	0	0	0
Underground Gas Storage	505	0	0	0	0	0	0	0	0	0	0	0	0	0	0	0
Compressor Station	601	25.27	4.073	0	5.109	0.393	0.651	1.497	0.008	1.303	7.685	0.020	0.562	0	0	46.57
Custom Treating Facility	611	0.006	0.001	0	0	0.000	0.000	0.001	0.000	0.003	0.002	0.000	0	0	0	0.013
Gas Gathering System	621	0.726	0	0	0	0	0	0	0	0	0	0	0	0	0	0.726
Meter Stations	MS	0	0	0	0	0	0.164	0	0	0	0	0	0	0	0	0.164
Tank Farms	TF	0.021	0.004	0	0	0.000	0.002	0.002	0.000	0.009	0.034	0.001	0	0	0	0.074
NGL Hub Terminal	676	0.002	0.000	0	0	0.000	0.000	0.000	0.000	0.001	0.001	0.000	0	0	0	0.003
Surface Waste Facility	701	0.015	0.003	0	0	0.000	0.001	0.002	0.000	0.007	0.005	0.001	0	0	0	0.034
Water Source	901	0.003	0.000	0	0	0.000	0.000	0.000	0.000	0.001	0.001	0.000	0	0	0	0.006
Water Source Battery	902	0.005	0.001	0	0	0.000	0.000	0.001	0.000	0.002	0.002	0.000	0	0	0	0.011
Wells	Gas	0.170	0.025	0	0	1.419	4.523	0.280	1.022	9.718	0.497	1.679	0.197	13.21	9.404	42.14
Wells	Oil	0.015	0.002	0	0	0.033	0.218	0.010	0.002	0.138	0.616	0.106	0	0.848	0.356	2.343
Wells	Water	0.006	0.001	0	0	0.014	0.024	0.004	0.001	0.058	0.018	0.044	0	0	0	0.170
Wells	Undefined	0.000	0.000	0	0	0.000	0.000	0.000	0.000	0.001	0.000	0.000	0	0	0	0.002
	Total	54.63	6.00	0.08	8.52	2.20	6.58	2.28	3.64	12.47	18.31	1.89	3.13	14.64	10.23	144.6

S3 Calculation of Methane Intensity / Leakage Rates

The methane intensities ("leakage rates") of marketed natural gas quoted in the manuscript were calculated by attributing emitted methane emissions to produced natural gas or oil on a per energy basis consistent with the Natural Gas Sustainability Initiative protocol (NGSI, 2021) and (Schneising et al., 2020). To facilitate fair comparisons among different sources, reported data were (re)calculated using a consistent set of assumptions as detailed in Table S7. Table S8 provides details of the methane intensity calculation for British Columbia based on the presently derived measurement-based inventory. Table S9 shows details of calculations for comparable intensities based on other cited methane measurements/estimates in the literature.

Table S7: Assumptions used to calculate methane intensities of produced gas.

Parameter	Assumed Value	Notes / Source
Energy Densities		
Canadian Products		
Natural Gas	0.03724 GJ/m³	Canadian Energy Regulator https://apps.cer-rec.gc.ca/Conversion/calculator-calculatrice.aspx?GoCTemplateCulture=en-CA
Light Crude Oil	38.51 GJ/m³	
Heavy Crude Oil	40.9 GJ/m³	
Condensate (Pentanes+)	35.17 GJ/m³	
Non-Upgraded Bitumen	42.8 GJ/m³	
Upgraded Bitumen (Synthetic Crude)	39.4 GJ/m³	
U.S. Products		
Oil	6004.3229 MJ/barrel	U.S. Energy Information Administration https://www.eia.gov/energyexplained/units-and-calculators/energy-conversion-calculators.php
Natural Gas	1,096,200 MJ/MMscf	
Unit Conversions		
Simple volume	0.028317 m³/cu.ft.	
U.S. oil and gas "standard" cubic feet (scf) to SI standard m³	0.028327 SI m³ / scf	Note U.S. "standard" oil and gas volume units are 60°F (288.71 K), 14.73 psia (101.5598 kPa) whereas SI standard conditions are 15°C (288.15 K) 101.325 kPa
Methane Density		
Density	0.678499 kg/m³	Ideal gas law at SI standard conditions (288.15 K, 101.325 kPa) with molecular mass = 16.043 kg/kmol
Methane Fraction		
British Columbia Natural Gas	85.2%	Chosen same as below for consistency
Methane fraction in U.S. Natural Gas	85.2%	Emission weighted fraction of NGSI defaults based on emissions breakdown in Table 1 of Alvarez et al. (2018)
U.S. Onshore Production	83.3%	(NGSI, 2021) Default Values
U.S. Gathering/Boosting	83.3%	
U.S. Processing	87.0%	
U.S. Transmission/Storage	93.4%	
U.S. Distribution	93.4%	

Table S8: Calculation of methane intensity of British Columbia marketed natural gas in 2021.

British Columbia 2021 Natural Gas Methane Intensity		**0.42% (0.37–0.48%)**
British Columbia 2021 Oil and Natural Gas Production		
BC 2021 Marketable Gas Production[1]	59,139,255,000 m^3	2,202,345,860 GJ
BC 2021 Oil Production[2]	676,614 m^3	26,056,421 GJ
BC 2021 Condensate Production (Pentanes+)[2]	5,889,278 m^3	207,125,918 GJ
Fraction of Produced Energy Attributed to Natural Gas Production		**0.904**
Assumed Methane Content of Produced Gas		85%
Produced Methane		**34,107 kt CH_4**
2021 Upstream Methane Inventory (Present Study)		144.6 (124–168) kt CH_4
Portion of Upstream Methane Emissions Attributable to Natural Gas		130.7 (112–152) kt CH_4
Natural Gas Methane Intensity (Upstream Sources Only)		0.38 (0.33–0.45) %
2020 Downstream Methane Inventory from ECCC (ECCC, 2022)		14.4 kt CH_4
Natural Gas Distribution		*3.8 kt CH_4*
Natural Gas Transmission & Storage		*10.2 kt CH_4*
Petroleum & Liquids Transport		*0.0 kt CH_4*
Petroleum Refining		*0.1 kt CH_4*
Other		*0.2 kt CH_4*
Portion of Downstream Methane Emissions Attributable to Natural Gas Production		13.0 kt CH_4
Total Estimated Oil & Gas Sector Methane Emissions		**159 (138–183) kt CH_4**
Portion of Total Methane Emissions Attributable to Natural Gas		**144 (125–165) kt CH_4**

[1] https://www.cer-rec.gc.ca/en/data-analysis/energy-commodities/natural-gas/statistics/marketable-natural-gas-production-in-canada.html

[2] https://www.cer-rec.gc.ca/en/data-analysis/energy-commodities/crude-oil-petroleum-products/statistics/estimated-production-canadian-crude-oil-equivalent.html

Table S9: Calculation of natural gas methane intensities from published measurements.

Estimate Derived from (Shen et al., 2022)	**Western Canada Natural Gas Methane Intensity (May 2018–Feb.2020)**		**0.87% (0.63–1.11%)**
	Western Canadian Oil and Gas Production		
	Marketed Gas Production[1]	163.174×10^9 m^3	6,077 PJ
	Light Crude[2]	34.262×10^6 m^3	1,319 PJ
	Heavy Crude[2]	23.547×10^6 m^3	963 PJ
	Condensate (Pentanes+)[2]	25.209×10^6 m^3	887 PJ
	Upgraded Bitumen[2]	64.036×10^6 m^3	2,741 PJ
	Non-Upgraded Bitumen[2]	108.065×10^6 m^3	4,258 PJ
	Fraction of Produced Energy Attributed to Natural Gas Production		**0.374**
	Assumed Methane Content of Produced Gas		85.2%
	Produced Methane		**94,328 kt CH_4**
	Shen et al. Methane Emissions Estimate (Shen et al., 2022)		**2200 (1600-2800) kt CH_4**
	Portion of Methane Emissions Attributable to Natural Gas Production		**823 (599–1047) kt CH_4**
	U.S. Natural Gas Methane Intensity (May 2018–Feb.2020)		**1.29% (1.08–1.51%)**
	U.S. Oil & Gas Production during May 2018-Feb. 2020 (measurement period of Shen et al., 2022)		
	Marketed Gas Production[1]	35,565,795 MMscf	38,987 PJ
	Light Crude[2]	4,372,613 Mbbl	26,255 PJ
	Fraction of Produced Energy Attributed to Natural Gas Production		**0.5976**
	Assumed Methane Content of Produced Gas		85.2%
	Produced Methane		**582.41 Mt CH_4**
	Shen et al. Methane Emissions Estimate (Shen et al., 2022)		**12.6 (10.5-14.7) Mt CH_4**
	Portion of Methane Emissions Attributable to Natural Gas Production		**7.53 (6.27–8.78) Mt CH_4**
Estimate Derived from (Alvarez et al., 2018)	**U.S. 2015 Natural Gas Methane Intensity**		**1.67% (1.45–1.94%)**
	U.S. 2015 Oil & Gas Production (Measurement/Estimation period of Alvarez et al., 2018)		
	Marketed Gas Production[3]	28,772,044 MMscf	31,540 PJ
	Crude Oil[4]	3,446,185 Mbbl	20,692 PJ
	Fraction of Produced Energy Attributed to Natural Gas Production		**0.374**
	Assumed Methane Content of Produced Gas		85.2%
	Produced Methane		**471.16 Mt CH_4**
	U.S. 2015 Methane Emissions Estimate (Alvarez et al., 2018)		**13 (11.3-15.1) Mt CH_4**
	Portion of Methane Emissions Attributable to Natural Gas Production		**7.85 (6.82–9.12) Mt CH_4**
Estimated Derived from (Schneising et al., 2020)	**Permian Basin 2018/2019 Natural Gas Methane Intensity**		**1.54% (0.99–2.09%)**
	Permian Basin 2018/2019 Oil & Gas Production (Measurement Period of Schneising et al., 2020)		
	Marketed Gas Production[3]	13,182 MMscf	14.5 PJ
	Crude Oil[4]	3897 Mbbl	23.4 PJ
	Fraction of Produced Energy Attributed to Natural Gas Production		0.382
	Assumed Methane Content of Produced Gas		85.2%
	Produced Methane		**78.79 Mt CH_4**
	Permian Estimate Derived from (Schneising et al., 2020)		**3.18 (2.05–4.31) Mt CH_4**
	Portion of Methane Emissions Attributable to Natural Gas Production		**1.21 (0.78–1.65) Mt CH_4**

Table S9: Calculation of natural gas methane intensities from published measurements *(continued)*

Estimated Derived from (Schneising et al., 2020)	**Bakken 2018/2019 Natural Gas Methane Intensity**		**1.47% (0.55–2.40%)**
	Bakken 2018/2019 Oil & Gas Production (Measurement Period of Schneising et al., 2020)		
	Marketed Gas Production[3]	2661 MMscf	2.92 PJ
	Crude Oil[4]	1361 Mbbl	8.17 PJ
	Fraction of Produced Energy Attributed to Natural Gas Production		**0.263**
	Assumed Methane Content of Produced Gas		85.2%
	Produced Methane		15.90 Mt CH_4
	Bakken Methane Estimate Derived from (Schneising et al., 2020)		**0.89 (0.33–1.45) Mt CH_4**
	Portion of Methane Emissions Attributable to Natural Gas Production		**0.23 (0.09–0.38) Mt CH_4**
	Appalachia Basin 2018/2019 Natural Gas Methane Intensity		**1.27% (0.80–1.75%)**
	Appalachia 2018/2019 Oil & Gas Production (Measurement Period of Schneising et al., 2020)		
	Marketed Gas Production[3]	30,312 MMscf	33.23 PJ
	Crude Oil[4]	127 Mbbl	0.76 PJ
	Fraction of Produced Energy Attributed to Natural Gas Production		**0.978**
	Assumed Methane Content of Produced Gas		85.2%
	Produced Methane		181.18 Mt CH_4
	Appalachia Methane Estimate Derived from (Schneising et al., 2020)		**2.36 (1.48–3.24) Mt CH_4**
	Portion of Methane Emissions Attributable to Natural Gas Production		**2.31 (1.45–3.17) Mt CH_4**
	Eagle Ford Basin 2018/2019 Natural Gas Methane Intensity		**1.63% (0.88–2.38%)**
	Eagle Ford 2018/2019 Oil & Gas Production (Measurement Period of Schneising et al., 2020)		
	Marketed Gas Production[3]	6674 MMscf	7.23 PJ
	Crude Oil[4]	1344 Mbbl	8.07 PJ
	Fraction of Produced Energy Attributed to Natural Gas Production		**0.476**
	Assumed Methane Content of Produced Gas		85.2%
	Produced Methane		**39.89 Mt CH_4**
	Eagle Ford Methane Estimate Derived from (Schneising et al., 2020)		**1.37 (0.74–2.00) Mt CH_4**
	Portion of Methane Emissions Attributable to Natural Gas Production		**0.65 (0.35–0.95) Mt CH_4**
	Anadarko Basin 2018/2019 Natural Gas Methane Intensity		**1.54% (0.99–2.09%)**
	Anadarko Basin 2018/2019 Oil & Gas Production (Measurement Period of Schneising et al., 2020)		
	Marketed Gas Production[3]	7421 MMscf	8.13 PJ
	Crude Oil[4]	548 Mbbl	3.29 PJ
	Fraction of Produced Energy Attributed to Natural Gas Production		0.712
	Assumed Methane Content of Produced Gas		85.2%
	Produced Methane		44.36 Mt CH_4
	Anadarko Basin Estimate Derived from (Schneising et al., 2020)		2.74 (2.00–3.48) Mt CH_4
	Portion of Methane Emissions Attributable to Natural Gas Production		1.95 (1.42–2.48) Mt CH_4
	Permian Basin 2018/2019 Natural Gas Methane Intensity		**4.40% (3.21–5.59%)**

1 https://www.cer-rec.gc.ca/en/data-analysis/energy-commodities/natural-gas/statistics/marketable-natural-gas-production-in-canada.html
2 https://www.cer-rec.gc.ca/en/data-analysis/energy-commodities/crude-oil-petroleum-products/statistics/estimated-production-canadian-crude-oil-equivalent.html
3 https://www.eia.gov/dnav/ng/hist/n9050us2a.htm
4 https://www.eia.gov/dnav/pet/hist/LeafHandler.ashx?n=PET&s=MCRFPUS1&f=A

S4 Statistical Testing of Emissions Variability

As discussed in the main text, statistical testing was performed to elucidate the temporal variability of detected sources in the aerial survey. With specific focus on workday-weekend variability as a surrogate of manual operations, two null hypothesis tests were deployed. This section describes the implementation of these tests and the results.

The first hypothesis test was performed on the subset of detected sources for which flights were performed on workday(s) *and* weekend(s). The difference(s) between flight-averaged emissions on the workday(s) and weekend(s) (Δ [kg/h]; positive if workday emissions exceeded weekend emissions and vice versa) were computed for each detected source. Available data for the parameter Δ were considered in aggregate – that is, across all sources – and for nine unique source categories: compressors and compressor buildings, dehydrators, flares (lit and unlit), piping infrastructure, power generators, separators, tanks, other (e.g., amine sweetening, line heater, fuel gas, wellhead, etc.), and unknown (not identifiable). One-sample t-tests were performed for each set of Δ data with the null hypothesis that the mean workday-weekend difference ($\overline{\Delta}$ [kg/h]) was zero (i.e., $H_o: \mu_\Delta = 0$; $H_a: \mu_\Delta \neq 0$). Results of the tests are summarized by source category in Table S10, which provides the size of the data set, the mean workday-weekend difference ($\overline{\Delta}$), the t-statistic, and p-value of the hypothesis test. The present data did not justify rejecting the null hypothesis for any source category at 5% significance, implying no statistically significant difference between workday and weekend emissions.

The one-sample t-test only identifies statistical significance with respect to the mean and therefore does not necessarily capture effects at the tails of the distribution, where emissions from events like manual liquid unloading could be expected to manifest. Thus, an additional hypothesis test was performed to compare the source *distributions* between detected emissions on workdays and weekends. This was accomplished using the two-sample Kolmogorov-Smirnov (KS) test, which was applied to the same source categories as the t-test. The two-sample KS test compares the empirical cumulative distribution functions (eCDFs) for two datasets – here, quantified emission rates of all sources detected on workdays or weekends – with the null hypothesis that the underlying data come from the same distribution. Letting $\hat{F}_{workday}(Q)$ and $\hat{F}_{weekend}(Q)$ represent the eCDFs at source rate Q, the test statistic (D) is simply the maximum difference between the eCDFs:

$$D = \max_{Q} \left| \hat{F}_{workday}(Q) - \hat{F}_{weekend}(Q) \right| \qquad \text{(S11)}$$

which follows a Kolmogorov distribution parameterized by the size of the workday and weekend datasets. The two-sample Kolmogorov-Smirnov test was implements in MATLAB® using the *kstest2* function; results of the test are summarized in Table S10. Like the t-test, the present data did not justify rejecting the null hypothesis for any source category at 5% significance. This additionally implies that there was no statistically significant difference in source rate distributions between workdays and weekends for all source categories.

Table S10: Summary of hypothesis testing of workday-weekend variability of sources. The tests reveal that the present data imply <u>no</u> statistically significant difference (at 5% significance) in source rate nor distribution between workdays and weekends, which act as a surrogate for manual operations.

Source Category	One-sample t-Test				Two-Sample Kolmogorov-Smirnov Test			
	Count	$\bar{\Delta}$ [kg/h]	*t-stat* *[−]*	*p-value*	*Count* Workday	*Count* Weekend	*D-stat* *[−]*	*p-value*
Compressors	96	-3.89	-1.76	0.08	281	208	0.11	0.12
Dehydrators	14	-1.18	-0.62	0.54	31	29	0.13	0.96
Flares (lit and unlit)	12	+18.4	+1.80	0.10	21	17	0.30	0.31
Piping infrastructure	8	+7.84	+1.44	0.19	9	12	0.53	0.07
Power generators	6	-1.40	-0.58	0.59	37	28	0.26	0.18
Separators	25	+0.18	+0.19	0.85	59	34	0.25	0.10
Tanks	40	-0.05	-0.03	0.98	83	52	0.15	0.41
Other[a]	19	+0.34	+0.18	0.86	59	35	0.19	0.35
Unknown[b]	11	-0.28	-0.15	0.89	40	15	0.22	0.63
All sources	231	-0.47	-0.40	0.69	620	430	0.07	0.14

[a] Examples of "other" source types include: line heaters, amine sweetening buildings, meter buildings, pump buildings, wellheads, fuel gas pumps/skids, heater buildings and heaters, etc.

[b] Unknown sources are those for which aerial imagery, satellite imagery, and/or plot plan were insufficient to accurately apportion the detected emission.

In combination, these statistical tests leverage the available data to identify that workday-weekend variability – and, hence, the effects of manual operation at surveyed facilities – were statistically insignificant. Nevertheless, no statistical test is fundamentally conclusive, and alternative data acquired at different times (considering diurnal and seasonal variations) could yield statistically significant variability or bolster the presently observed insignificance.

S5 References

AER, 2018. Manual 015: Estimating Methane Emissions. Alberta Energy Regulator (AER).

Alvarez, R.A., Zavala-Araiza, D., Lyon, D.R., Allen, D.T., Barkley, Z.R., Brandt, A.R., Davis, K.J., Herndon, S.C., Jacob, D.J., Karion, A., Kort, E.A., Lamb, B.K., Lauvaux, T., Maasakkers, J.D., Marchese, A.J., Omara, M., Pacala, S.W., Peischl, J., Robinson, A.L., Shepson, P.B., Sweeney, C., Townsend-Small, A., Wofsy, S.C., Hamburg, S.P., 2018. Assessment of methane emissions from the

U.S. oil and gas supply chain. Science (80-.). 361, 186–188. https://doi.org/10.1126/science.aar7204

BCOGC, 2022a. Facility Locations (Permitted) [WWW Document]. URL https://data-bcogc.opendata.arcgis.com/datasets/5ace26f614b9435492d679d766430143_0 (accessed 10.18.22).

BCOGC, 2022b. Facility Locations (Pre-2016) [WWW Document]. URL https://data-bcogc.opendata.arcgis.com/datasets/e2014a76454545abb0509afa2444876b_0 (accessed 10.18.22).

BCOGC, 2022c. Well Surface Hole Locations (Permitted) [WWW Document]. URL https://data-bcogc.opendata.arcgis.com/datasets/9149cb556e694617970a5774621af8be_0 (accessed 10.18.22).

Clearstone Engineering Ltd., 2018. Update of Equipment, Component and Fugitive Emission Factors for Alberta Upstream Oil and Gas. Alberta Energy Regulator (AER).

Conrad, B.M., Tyner, D.R., Johnson, M.R., 2022. Robust Probabilities of Detection and Quantification Uncertainty for Aerial Methane Detection: Examples for Three Airborne Technologies. Remote Sens. Environ. https://doi.org/https://doi.org/10.31223/X5S05F

D'Antoni, M.D., 2018. Level Controller Emission Study Fisher L2 and Improved Relays Norriseal 1001A and EVS. Petroleum Technology Alliance of Canada (PTAC).

ECCC, 2022. 2020 National Inventory Report (NIR) - Part 3. Environment and Climate Change Canada (ECCC).

Government of Alberta, 2020. Quantification Protocol for Greenhouse Gas Emission Reductions from Pneumatic Devices - Version 2.1.

Johnson, M.R., Tyner, D.R., Conrad, B.M., 2022. Root Causes of Oil and Gas Sector Methane Emissions: On-Site Investigations of Aerial Measured Sources. Environ. Sci. Technol.

NGSI, 2021. NGSI Methane Emissions Intensity Protocol Version 1.0. Natural Gas Sustainability Initiative (NGSI).

Petrinex, 2022a. British Columbia Public Data [WWW Document]. URL https://www.petrinex.ca/PD/Pages/default.aspx (accessed 10.15.22).

Petrinex, 2022b. Petrinex Activity Codes (British Columbia) [WWW Document]. URL https://www.petrinex.gov.ab.ca/bbreportsBC/PRAActivityCodes.htm (accessed 10.18.22).

Prasino Group, 2013. Final Report for Determining Bleed Rates for Pneumatic Devices in British Columbia. Report to British Columbia Ministry of the Environment.

Robinson, C., Driver, K., D'Antoni, M.D., 2018. Cap-Op Energy British Columbia Oil and Gas Methane Emissions Field Study. https://doi.org/https://www.bcogc.ca/files/resources/bc-cas-mefs-chapters-1-3-err2-20200224.pdf

Schneising, O., Buchwitz, M., Reuter, M., Vanselow, S., Bovensmann, H., Burrows, J.P., 2020. Remote sensing of methane leakage from natural gas and petroleum systems revisited. Atmos. Chem. Phys. 20, 9169–9182. https://doi.org/10.5194/acp-20-9169-2020

Shen, L., Gautam, R., Omara, M., Zavala-Araiza, D., Maasakkers, J.D., Scarpelli, T.R., Lorente, A., Lyon, D., Sheng, J., Varon, D.J., Nesser, H., Qu, Z., Lu, X., Sulprizio, M.P., Hamburg, S.P., Jacob, D.J., 2022. Satellite quantification of oil and natural gas methane emissions in the US and Canada including contributions from individual basins. Atmos. Chem. Phys. 22, 11203–11215.

https://doi.org/10.5194/acp-22-11203-2022

Sitter, R.R., 1992. A resampling procedure for complex survey data. J. Am. Stat. Assoc. 87, 755–765. https://doi.org/10.1080/01621459.1992.10475277

Tyner, D.R., Johnson, M.R., 2021. Where the Methane Is—Insights from Novel Airborne LiDAR Measurements Combined with Ground Survey Data. Environ. Sci. Technol. 55, 9773–9783. https://doi.org/10.1021/acs.est.1c01572

Western Climate Initiative, 2013. WCl Quantification Method 2013 Addendum to Canadian Harmonization Version.